Comparison of near−surface air temperatures and MODIS ice−surface temperatures at Summit, Greenland (2008–2013)

Christopher A. Shuman[1], Dorothy K. Hall[2], Nicolo E. DiGirolamo[3], Thomas K. Mefford[4], and Michael J. Schnaubelt[5]

[1]University of Maryland, Baltimore County, Joint Center for Earth Technology, NASA GSFC, Greenbelt, Maryland, USA (christopher.a.shuman@nasa.gov)

[2]Cryospheric Sciences Laboratory, NASA GSFC, Greenbelt, Maryland, USA (dorothy.k.hall@nasa.gov)

[3]Science Systems and Applications, Inc., NASA GSFC, Greenbelt, Maryland, USA (nicolo.e.digirolamo@nasa.gov)

[4]Cooperative Institute for Research in Environmental Sciences, University of Colorado at Boulder, and NOAA Earth System Research Laboratory, Boulder, Colorado, USA (thomas.mefford@noaa.gov)

[5]University of Maryland, Baltimore County, Joint Center for Earth Technology, Baltimore, Maryland, USA (sc6@umbc.edu)

Abstract

We have investigated the stability of the MODerate−resolution Imaging Spectroradiometer (MODIS) ice−surface temperature (IST) product from Terra for use as a climate−quality data record. The availability of climate−quality air temperature data (T_A) from a NOAA observatory at Greenland's Summit station has enabled this high−temporal resolution study of MODIS ISTs. During a >5 year period (July 2008 to August 2013), more than 2500 IST values were compared with ±3-minute average T_A

values from NOAA's primary 2 m temperature sensor. This enabled an expected small offset between air and ice sheet surface temperatures (T_A > IST) to be investigated over multiple annual cycles. Our principal findings show that: 1) IST values are slightly colder than the T_A values near freezing but this offset increases as temperature decreases; and 2) there is a pattern in IST−T_A differences as the solar zenith angle (SoZA) varies annually. This latter result largely explains the progressive offset from the in situ data at colder temperatures but also indicates that the MODIS cloud mask is less accurate approaching and during the polar night. The consistency of the results over each year in this study indicates that MODIS provides an alternative platform for remotely deriving surface temperature data, with the resulting IST data most compatible with in situ T_A data when the sky is clear and SoZA is less than ~85 degrees. The ongoing IST data set should benefit from improved cloud filtering as well as algorithm modifications to account for the progressive offset from T_A at colder temperatures.

1. Introduction

There has been a great deal of attention on the increasing melt on Greenland especially related to recently-observed warm events and associated unusual climate conditions (Nghiem et al. 2012; Hall et al. 2013; Hanna et al. 2013), the positive ice−albedo feedback (Box et al. 2012), and overall climate conditions (Steffen and Box, 2001; Rennermalm et al. 2013). Climate models predict continued Arctic warming but they differ in their predictions of the extent, rate and magnitude of the temperature increases. The most practical way to get a spatially−broad and temporally−extensive

measurement of surface temperature for an area the size of the Greenland Ice Sheet (GrIS) is through satellite remote sensing given the difficulties of operating equipment reliably in harsh polar conditions. However, the uncertainties in satellite–derived ice surface temperatures (ISTs) must be assessed relative to independent T_A data sets such as those from well–calibrated automatic weather stations (AWS) to validate them for use in climate studies. Full confidence in these remote-sensing records can be established by comparison to the best available in situ climate data.

This research provides an additional assessment of the uncertainties in these multi–year MODIS-derived surface temperatures. Preliminary results have been presented in Hall et al. (2008a and 2012) and Koenig and Hall (2010) for a restricted period of time and temperature range. In those studies, a 1 to 3°C 'cold bias' was identified at Summit using thermocrons (e.g. small temperature loggers) placed on the snow surface during the winter of 2008/09 (Koenig and Hall, 2010). In the present work, we assess satellite–derived "clear–sky" IST data from the MODerate–resolution Imaging Spectroradiometer (MODIS) near Summit Station, Greenland (http://modis-snow-ice.gsfc.nasa.gov/index.php?c=greenland). These IST data from July 2008 through August 2013 are compared to 2 m T_A data from the Temporary Atmospheric Watch Observatory (TAWO). This facility has been operated at Summit Station since 2005 by the NOAA Earth System Research Laboratory's (ESRL) Global Monitoring Division (GMD) (http://www.esrl.noaa.gov/gmd/obop/sum/). This analysis approach is justified even though air and surface temperatures are not the same (e.g. Hudson and Brandt, 2005) because of the quality and high temporal resolution of the NOAA T_A data.

The overlap period between the MODIS and NOAA Logan temperature records began at Summit in July 2008 (see Table 1) and is ongoing.

2. Background

Surface and air temperatures on the GrIS have been studied on the ground using automatic weather station (AWS) data (e.g. Steffen and Box 2001; Shuman et al. 2001; Box 2002; van den Broeke et al. 2008, 2011) and using satellite data (e.g. Key and Haefliger 1992; Haefliger et al. 1993; Stroeve and Steffen 1998; Comiso et al. 2006; Wang and Key 2005a,b; Comiso 2006; Hall et al. 2008a,b; Lampkin and Peng 2008; Hall et al. 2009, 2013). Modeling results are also available (e.g., van den Broeke et al. 2011; Cullather et al. in press) as well as reanalysis products that ingest data from some in situ sensors (Lucas-Picher et al. 2011). For a variety of reasons, including the remote and difficult environment, calibration, equipment maintenance, and or power limitations, deriving accurate, extensive, and internally−consistent climate−quality temperature records for ice sheet locations remains a challenge.

IST has been derived from IR channels on various satellites. The primary instruments for which such IR data have been available are the Advanced Very High Resolution Radiometer (AVHRR) on NOAA's Polar−orbiting Operational Environmental Satellites (POES) and MODIS on NASA's Terra and Aqua satellites as well as Landsat-7's, Enhanced Thematic Mapper Plus (ETM+, Band 6) and also Terra's Advanced Spaceborne Thermal Emission and Reflection Radiometer (ASTER). These sensors have been recently been augmented by the Visible Infrared Imaging Radiometer Suite

(VIIRS) instrument on the Suomi NPP (National Polar−orbiting Partnership) satellite and the Thermal Infrared Sensor (TIRS) on Landsat 8.

Hall et al. (2008a) documented that the orbiting IR sensor data available at that time from ETM+, ASTER, and MODIS had very similar performance on the GrIS with a MODIS RMS error of 2.1°C. However, the clear−sky limitation of satellite−derived IR temperatures precludes the measurement of the surface under all−weather conditions. Cloud−top temperatures tend to be colder than surface temperatures because air temperatures tend to fall through the lower atmosphere with increasing altitude (Westermann et al., 2012). Further, orbit characteristics of each satellite allow particular locations to be sampled only during a specific period on any given day. The surface temperature of the ice sheet beneath clouds can be very different, usually higher, from that under clear skies (e.g. Miller 1956; Stroeve and Steffen 1998; Hudson and Brandt 2005) especially in the winter when there are inversions in the lower atmosphere (Miller et al., 2013). Thus a time series of satellite−derived, clear sky, surface temperatures can be significantly different from an all−conditions surface temperature record (Liu et al. 2009; Koenig and Hall, 2010). Initial comparisons between IST and snow surface temperature data from thermochrons (a type of programmable thermistor) are presented in Koenig and Hall (2010) and Hall et al. (2012). Those comparisons of temporally−similar temperatures during November 2008 to February 2009, identified a ~3°C 'cold bias' in the IST data for Summit. Hudson and Brandt (2005) documented a similar offset using in situ data in Antarctica.

2a. NOAA 2 m Air Temperatures

Although preceded by a series of AWS installed in support of the Greenland Ice Sheet Program 2 (GISP2), deep core and ancillary research projects (Stearns, 1996; Shuman et al. 2001), climate−quality measurements began in 2005 after the GISP2 camp became Summit Station and also a year−round research facility. Though preliminary measurements began in 2005, NOAA began operating the Temporary Atmospheric Watch Observatory (TAWO) facility as part of its Global Monitoring Division (GMD) in 2007. GMD initially used a Vaisala sensor in an aspirated Met One housing at TAWO. In July 2008, a more accurate Logan temperature sensor was installed and now operates in parallel with the Vaisala sensor at TAWO; both sensors are currently in aspirated Cambridge housings. At Summit, as at its other GMD sites, NOAA utilizes a Logan Enterprises PT139 sensor that is factory calibrated using industry-traceable equipment across the expected temperature range for the site (http://www.loganent.com/products.php?p=32 see 'Platinum Sensor Data'). Further, using International Temperature Scale of 1990 (ITS-90) standards, NOAA GMD protocols are then applied across the resistances corresponding to a temperature range of -75°C to +5°C to achieve temperature accuracies of better than 0.1°C which are then rounded off to this resolution for the Summit data. Operationally, the sensors acquire T_A data four times every minute and those values are averaged to 1 minute and, as in this study, more typically for longer periods. On−site personnel are scheduled to maintain the temperature sensors on a daily basis to ensure proper ventilation and the sensor arm is raised every year to maintain the 2 m offset from the ice sheet surface. The availability of power year−round at the station means that these

sensors can be continually ventilated as opposed to most AWS temperature sensors which are typically not ventilated. However, there may be occasional brief impacts due to power or other equipment problems. Active ventilation of the T_A sensors avoids some data–quality issues such as solar heating during periods of low wind speed and high solar insolation that have been quantified for more typical but passively–ventilated AWS temperature sensors used on ice sheets (Shuman et al. 2001; Genthon et al. 2011).

2b. MODIS Ice Surface Temperatures

The IR–derived temperatures from MODIS or other sensors (e.g. Key and Haefliger, 1992; Comiso 2006; Hall et al. 2008) represent a skin temperature not an air temperature. Skin temperature is the temperature of the surface at radiative equilibrium or the temperature essentially at the interface between the snow/ice surface and the atmosphere for a site like Summit Station (Warren and Brandt, 2008). This explains some of the differences between IST and T_A identified in this study and discussed further below. As described in detail by Hall et al. (2012), IST can be mapped at 1–km resolution using data from two nearly-identical MODIS instruments on the Terra and Aqua satellites. The present study uses only the Terra satellite's Collection 5 MOD29 IST data. The MOD29 algorithm was developed to measure IST of snow and ice based on the AVHRR heritage algorithm of Key and Haefliger (1992). MOD29 had been used successfully to map IST of sea ice but all land had been masked out. As a special product (Hall et al., 2012; 2013), the land/water mask was adjusted and now provides IST data using the MOD29 algorithm over Greenland as well as over sea ice. Improved

geolocation data for the IST pixels was obtained using the MOD03 product. The Greenland data are available from: http://modis-snow-ice.gsfc.nasa.gov/. For further information, see Hall et al. (2004) or Riggs et al. (2006) as well as additional documentation at: https://nsidc.org/data/docs/daac/modis_v5/mod29_modis_terra_seaice_5min_swath_1km.gd.html.

The Greenland IST data uses the standard MODIS 1–km resolution cloud mask (MOD35) that uses up to 14 spectral bands and multiple spectral and thermal tests to identify clouds (Ackerman et al. 1998, 2008; Liu et al. 2004). This product uses several cloud–detection tests to indicate a level of confidence that a pixel is clear or cloudy. For the MODIS data used in this study, changes were implemented resulting in improvement in cloud masking during the polar night over snow and ice targets (Frey et al. 2008). These changes reduced the misidentification of cloud as clear but did not change the misidentification of clear pixels as cloud–covered (Liu et al. 2004; Frey et al. 2008; Westermann et al. 2012; Østby et al. 2014). For the Greenland IST data near Summit used here, the conservative cloud tests in MOD35, called 'confident clear', are used but have been considered to be overly conservative over snow and ice targets (Stroeve et al. 2006). However, Hall et al. (2013) documents the need for additional editing of 'clear' pixels that are too cold due to the presence of undetected clouds in the MOD35 product. It is worth noting that of the 1883 days in the study period, ~29% had no IST values for Summit, ~19% of the days had one IST value, ~35% of the days had two IST values, and ~17% of the days had three IST values (2536 IST values total).

185

186 **3. Methodology and Results**

187 The Terra MODIS–derived IST data set (Riggs et al. 2006) and associated swath
188 geolocation data were used to identify values that passed the 'confident–clear' test and
189 were up to 3 km from the TAWO location. If multiple IST values were within this
190 distance, only the closest observation was included in the data set. These data were
191 extracted for July 2008 through August 2013. Using the 1–minute average data from
192 TAWO, ±3-minute average T_A measurements were derived to bracket the times of the
193 MODIS ISTs. This averaging period was chosen to provide a close correspondence to
194 the well–defined data acquisition times from MODIS. All data are recorded in UTC.
195 Following some quality–control tests to identify possibly inaccurate T_A values, typically
196 associated with equipment issues at TAWO (only one 1-minute data value was
197 removed by looking for unusual excursions in the 1-minute averages within the NOAA
198 time series but a small number of other days were reprocessed), the combined data set
199 was temporally aligned and then analyzed. In addition, the IST data were analyzed
200 without and with a filter as discussed further below, that was designed to minimize the
201 impact of expected cloud-impacted values. In the following material, all data from 2008
202 to 2013 is plotted collectively but individual years are summarized in Table 1.

203

204 ***3a. T_A and IST Data 2008-2013***

205 The relationship between the ±3-minute average T_A and the contemporaneous IST data
206 is shown in Figure 1 for more than 2500 temperature comparisons. The red +'s
207 represent the full data set in the scatter plot and show a fairly strong linear

relationship across the temperature range of approximately 0 to less than −60°C. Note, this upper limit would obscure the positive temperatures associated with the rare melt event(s) in 2012 at Summit during the July 11-12, 2012. The trend of the regression line through all the matched temperature values indicates that the expected slightly colder IST values range from just colder than the T_A observations at the upper part of the temperature range to about 5°C colder at the lower part of the Greenland Summit's temperature range. As shown in Figure 1, a number of outliers scatter significantly (> 10°C) from the overall trend of the full data set.

Because of this degree of scatter, it appears that some of the IST data are still cloud−impacted or are otherwise anomalous despite the 'confident clear' cloud masking procedure. Examination of Figure 1 suggests that these outliers can be present throughout the annual temperature range. Generally, IR−derived values impacted by clouds will be substantially colder than the underlying ice sheet surface especially in the summer months (Hall et al. 2013) although there are some instances where the IST is slightly warmer than the corresponding T_A value possibly as a result of mixing of warmer air from aloft during storms (Koenig and Hall, 2010; Miller 1956). While it is possible that some of the scatter is due to the in situ data, the NOAA Logan T_A sensor has been calibrated to ITS-90 standards using NOAA's protocols with reported temperatures at ±0.1°C accuracy. In addition, the standard deviations of all the 1−minute data used in the ±3-minute averages in this study are typically (~98% of the time) less than 0.5°C (Figure 2). The scatter shown in Figure 2 indicates that temperature variability is more common at lower temperatures. The standard

231 deviations were not plotted as error bars in Figure 1 because most would not be
232 visible. Table 1 provides an overall assessment of the uncertainty of the IST data
233 relative to the T_A data.
234
235 To better resolve the expected 'cold bias' in the IST values, a filter was applied to
236 reduce the overall variability in the data set. To dramatically reduce cloud–impacted
237 and other anomalous IST values, an IST–T_A ±5-degree filter based on the full data set's
238 linear regression was applied to the full data set. This range was selected to leave the
239 majority of the data available for the additional steps in the analysis but without
240 unevenly influencing any part of the overall data range. The points that were within
241 this filter range are indicated with blue x's in Figure 1 and are represented by the blue
242 regression line. Both data sets, 'all' and 'filt.' are summarized in Figure 1 with IST–T_A
243 difference statistics. Inspection of Figure 1 indicates this filter eliminates a number of
244 outliers, most that are too cold but also some that are apparently too warm, from the
245 remainder of the analysis (i.e. points with red +'s only). The resulting blue linear
246 regression line does not differ markedly from the initial regression through the raw
247 data but the filtering does reduce the mean difference by 0.75°C and the variability is
248 also reduced (see Figure 1 and also the year-by-year data in Table 1). The filtered data
249 set is smaller by ~10% and is used for the rest of the study.
250
251 During our quality control assessment of the NOAA T_A data, we observed that strong
252 (>4°C) temperature changes can occur within some of the study's ±3-minute averaging
253 periods (see Figure 2). These brief temperature swings can cause the standard

deviation of the values to approach 2°C in some cases. Close examination of the minute-by minute temperature data for the study period only identified one clearly anomalous 1-minute observation that was edited from the NOAA time series. However, due to this analysis, 20 days worth of T_A data were identified out of a total of 1883 days in the study period and reprocessed to account for minor data issues. In any case, it is important to document that T_A can fluctuate relative to the essentially instantaneous IST data and this may account for a minor amount of the scatter observed in Figure 1.

3b. MODIS IST Variables

We used a number of ancillary parameters that are part of the MOD29 IST product in this study. First, we assessed the variability in IST−T_A differences due to the distance between the image pixel and the in situ values. As noted previously, offsets up to 3 km from the in situ data were accepted as in some cases, the IST value over TAWO was not available typically due to the cloud mask. Figure 3 shows the IST−T_A differences for 2008−2013 as a function of the offset distance. A weak relationship is indicated by the regression line with the plot suggesting that most of the variability in the temperature differences is not a function of distance given the substantial variability within the 1 km distance from TAWO alone indicated in Figure 3. It is important to note that elevation variation is very small in the region based on unpublished ground-based GPS surveys conducted by Summit Station staff. The ice sheet area around Summit has a homogeneous surface as noted by Koenig and Hall (2010).

The senor's view zenith angle (SeZA) was also investigated because it can influence the IST−T_A difference.. MODIS has a swath width of 2330 km, therefore IST values for a specific location can be derived over a range of viewing geometries as the sensor orbits the Earth. The sensor's SeZA is always recorded as a positive number as shown in Figure 4. The 2008−2013 data suggest that slightly colder IST values are derived at larger angles from zenith. Results from previous research using AVHRR data (Dozier and Warren, 1982) showing a temperature variation with SeZA are compatible with the results here. However, because SeZA relative to a site like Summit is a function of satellite orbit and does not vary as a function of temperature through the year, this factor may contribute scatter but does not cause the overall cold bias apparent in Figure 1.

The influence of the solar zenith angle (SoZA) on MODIS surface-temperature retrievals was also investigated.. A progressively-greater offset between the IST and Summit station temperatures toward the lower end of the temperature range (Figure 1) suggests that the IST calibration at the low temperatures may be suspect. This is also illustrated in Figure 5 with the 2008−2013 IST−T_A differences plotted as a function of SoZA. Given Summit's northern latitude (72.58°N), this parameter varies considerably through the year with values >90 degrees indicating that the sun is below the horizon as is expected during the polar night. The trend of all these data is also fairly consistent in each year of the study and shows colder IST values relative to T_A (more negative differences) as a function of higher SoZAs. Crucially, the magnitude of this regression (i.e. the offset of the temperature difference across the range of

SoZA,~4°C) is quite close to the magnitude of the progressive IST cold bias observed in Figure 1 with the offset increasing as temperatures fall over the temperature range expected during an annual cycle.

In addition, as shown by the data plotted in Figure 5 and similarly for each year in the study, there appears to be more variability in IST-T_A differences about the trend at larger SoZAs. In fact, the linear regression mostly serves to illustrate the variation in the relationship of SoZA and temperature difference relative to the change from 'day' to 'night' cloud filtering algorithms in the MODIS processing stream. Ackerman et al. (1998) document that the cloud–masking algorithm changes from day–mode to night–mode when SoZA exceeds 85 degrees. This is close to where the data points in Figure 5 changes from having a fairly distinct linear trend despite some scattered values (<80 degrees) although it is steeper than the overall regression and begins to show increased variability (>80 degrees). Even though the difference values continue to be generally–to–strongly negative at SoZAs greater than ~80 degrees, the overall increase in scatter in Figure 5 corroborates the known issue that the cloud–clearing algorithm is less reliable in near–to–total darkness. This relationship within the filtered data set likely contributes to the cold bias observed in Figure 1 as SoZA does vary across the annual temperature cycle. This becomes especially problematic when monthly-average ISTs are investigated because the higher temperatures (which can occur under cloud cover) will not consistently be retrieved by MODIS due to cloud cover obscuration of the surface (Hall et al., 2012).

4. Discussion

The multi-year comparisons presented here document that the observed 'cold bias' (e.g. Figure 1; Hall et al. 2008, Figure 5) is not a static offset between T_A and IST over the full annual temperature range observed at Summit Station. The offset between contemporaneous air and ice surface values is progressive across the full annual temperature range. It ranges from about −0.5°C at the upper end of the temperature range and increases to as much as −5°C at −60°C after applying a modest additional test to reduce cloud-impacted IST values. Further, this analysis reproduces a reported ~3°C cold bias between MODIS-derived skin and NOAA air temperatures (Koenig and Hall, 2010) observed with data acquired from mid−November 2008 to mid−February 2009. Finally, our analysis of ancillary IST parameters confirms a reason for the observed increasing cold bias as a function of decreasing temperatures at the Summit, Greenland site. The combined impact of SoZA and reduced accuracy of cloud masking during the polar night appears to explain the overall observed cold bias (Figure 5).

Work by Hudson and Brandt (2005) suggests that inversions can produce significant temperature gradients between the T_A sensor (nominally height of 2 m) and the ice surface but it is not clear that these results are applicable to central Greenland. Work by Miller et al. (2013) at Summit indicates that there are variations in the frequency and intensity of inversions at Summit but do not detail their impact very close to the surface or other factors that can influence near-surface inversions. Our results (Figure 1) suggest that while a seasonally-varying 'inversion effect' may be a factor it seems unlikely to lead to the rather smooth progression of the offset between IST and T_A

values over the annual temperature range. Therefore, the progressive cold bias detailed in this analysis appears to be primarily a function of the SoZA when the MODIS data is acquired. A secondary factor appears to be the reduced ability to mask out cloudy, and generally colder, MODIS pixels by the cloud–masking portion of the MOD29 algorithm; this becomes more common when the sun is close to or below the horizon. The effectiveness of the cloud–masking algorithm is reduced when it changes from 'day' to 'night' mode when SoZA's exceed 85 degrees (Ackerman et al. 1998) and this is apparent in both the unfiltered and filtered temperature difference data. This suggests that improved cloud masking , though challenging during the polar night, would substantially improve the derived IST values for most users. Lesser factors such as the distance between the IST value and the in situ temperature site or the MODIS SeZA relative to the in situ data contribute some scatter to the IST to T_A relationship but do not control the progressive cold bias.

5. Conclusions

Analysis of the relationship between the TAWO 2 m T_A data and MODIS-derived IST values confirms that there is a progressive 'cold bias' between the temporally-coincident air and ice surface observations near the GrIS's Summit Station. In addition, for temperatures that are closer to 0°C, IST values are closely compatible with contemporaneous (±3-minute) T_A data. These data sets, compared during the period from 2008–2013, show that there is a difference of about −0.5°C at the upper end of the temperature range that increases to as much as −5°C at −60°C. The offset is within the IST uncertainty at the upper end of the temperature range with a larger offset and

colder IST values relative to T_A averages increasing progressively over the annual temperature range This offset appears to be largely a function of the MODIS data's SoZA and, perhaps to a lesser degree, the ability to reliably identify cloud–impacted pixels by the cloud–masking algorithms. The impact of temperature inversions that can cause near-surface temperature gradients remains uncertain (e.g. Miller et al., 2013) and would assessing their impact would require additional high-resolution observations at TAWO. The analysis results are consistent in each year of the study and are consistent with previous results obtained at Summit by Koenig and Hall (2010). The consistency of the relationship between T_A and IST suggests that an empirical correction may be used to refine the overall IST values to make them more compatible with T_A observations. Other sensors with IR bands, such as VIIRS and TIRS, would benefit from similar comparisons to NOAA's climate–quality temperature observations at the Greenland Summit. Finally, although we have identified some issues that IST users should consider, the bottom line is that the satellite IST observations have the consistency to provide knowledge of surface temperature of the GrIS useful for climate-modeling and climate-change studies.

Acknowledgements

The authors would like to thank the support staff at the Greenland Summit Station for helping to provide the in situ data necessary for this study. The T_A data were derived from NOAA's Earth System Research Laboratory, Global Monitoring Division data sets. NASA's Cryospheric Sciences Program provided funding for the MODIS IST dataset as well as the work performed at NASA GSFC and at UMBC. Jack Xiong, Brian Wenny of the

391 MODIS Characterization and Support Team, and George Riggs (SSAI at GSFC) provided
392 additional insights on the IST data and MODIS products. We thank the Editor and three
393 anonymous reviewers for their comments and guidance that improved the final paper.
394

395 **References**

396 Ackerman, S.A., K.I. Strabala, P.W.P. Menzel, R.A. Frey, C.C. Moeller, and L.E. Gumley,
397 1998: Discriminating clear sky from clouds with MODIS. *J. Geophys. Res.,* **103,** D24,
398 32,141–32,157.
399 Ackerman, S.A., R.E. Holz, R. Frey, E.W. Eloranta, B. Maddux, and M. McGill, 2008. Cloud
400 detection with MODIS. Part II: Validation. *J. Atmos. Ocean. Tech.* **25**, 1073–1086.
401 Box, J.E., 2002: Survey of Greenland instrumental temperature records: 1873–2001.
402 *Int. J. Climatol.,* **22**, 1829–1847.
403 Box, J.E., X. Fettweis, J.C. Stroeve, M. Tedesco, D.K. Hall, and K. Steffen, 2012: Greenland
404 ice sheet albedo feedback: thermodynamics and atmospheric drivers, *The Cryosphere,*
405 **6**, 821–839.
406 Comiso, J.C., 2006: Arctic warming signals from satellite observations. *Wea.,* **61**, 3,
407 70–76.
408 Cullather, R.I., S.M.J. Nowicki, B. Zhao, and M.J. Suarez, 2014: Evaluation of the surface
409 representation of the Greenland Ice Sheet in a general circulation model, *J. Clim.,* (in
410 review).
411 Dozier, J., and S. Warren, 1982: Effect of viewing angle on the infrared brightness
412 temperature of snow. *Wat. Res. Res.,* **18,** 5, 1424–1434.

413 Frey, R., S. Ackerman, Y. Liu, K. Strabala, H. Zhang, J. Key, and X. Wang, 2008: Cloud
414 detection with MODIS. Part I: Improvements in the MODIS cloud mask for collection
415 5. *J. Atm. Ocean. Tech.,* **25**, 1057–1072.
416 Genthon C, Six D, Favier V, Lazzara M, Keller L., 2011: Atmospheric temperature
417 measurement biases on the Antarctic Plateau. *J. Atm. Ocean. Tech.,* **28**, 1598–1605.
418 Hall, D.K., J. Key, K.A. Casey, G.A. Riggs, and D.J. Cavalieri, 2004: Sea ice surface
419 temperature product from MODIS. *IEEE Trans. Geosc. Rem. Sen.,* **42**, 1076–1087.
420 Hall, D.K., J.E. Box, K.A. Casey, S.J. Hook, C.A. Shuman, and K. Steffen, 2008a: Comparison
421 of satellite−derived ice and snow surface temperatures over Greenland from MODIS,
422 ASTER, ETM1 and in−situ observations. *Rem. Sens. Environ.,* **112**, 3739–3749.
423 Hall, D.K., R.S. Williams Jr., S.B. Luthcke, and N.E. DiGirolamo, 2008b: Greenland Ice
424 Sheet surface temperature, melt and mass loss: 2000–2006. *J. Glac.,* **54**, 81–93.
425 Hall, D.K., S.V. Nghiem, C.B. Schaaf, N.E. DiGirolamo, and G. Neumann, 2009: Evaluation
426 of surface and near−surface melt characteristics on the Greenland Ice Sheet using
427 MODIS and QuikSCAT data. *J. Geophys. Res.,* **114**: F04006.
428 Hall, D.K., J.C. Comiso, N.E. DiGirolamo, C.A. Shuman, J.R. Key, and L.S. Koenig, 2012: A
429 satellite−derived climate−quality data record of the clear−sky surface temperature of
430 the Greenland Ice Sheet, *J. Clim.,* **25**, 4785–4798.
431 Hall, D.K., J.C. Comiso, N.E. DiGirolamo, C.A. Shuman, J.E. Box, and L.S. Koenig, 2013:
432 Variability in the surface temperature and melt extent of the Greenland ice sheet
433 from MODIS, *Geophys. Res. Lett.,* **40**, 1–7.
434 Hanna, E., X. Fettweis, S.H. Mernild, J. Cappelen, M.H. Ribergaard, C.A. Shuman, K.
435 Steffen, L. Wood, and T.L. Mote, 2013: Atmospheric and oceanic climate forcing of the

436 exceptional Greenland ice sheet surface melt in summer 2012, *Int. J. Climatol.,* **34**, 4,
437 1022–1037.
438 Hudson, S.R., and R.E. Brandt, 2005: A look at the surface−based temperature inversion
439 on the Antarctic Plateau. *J. Clim.,* **18**, 1673–1696.
440 Key, J., and M. Haefliger, 1992: Arctic ice surface temperature retrieval from AVHRR
441 thermal channels. *J. Geophys. Res.,* **97**, D5, 5885–5893.
442 Koenig, L.S., and D.K. Hall, 2010: Comparison of satellite, thermochron and station
443 temperatures at Summit, Greenland, during the winter of 2008/09. *J. Glac.,* **56**, 735–
444 741.
445 Liu, Y., J. Key, R. Frey, S. Ackerman, and W.P. Menzel, 2004: Nighttime polar cloud
446 detection with MODIS. *J. App. Meteor.,* **92**, 181–194.
447 Liu, Y., J. Key, and X. Wang, 2009: Influence of changes in sea ice concentration and
448 cloud cover on recent Arctic surface temperature trends. *Geophys. Res. Lett.,* **36**,
449 L20710.
450 Lucas-Picher, P., M. Wulff-Nielsen, J.H. Christensen, G. Aðalgeirsdóttir, R. Mottram, and
451 S.B. Simonsen, 2012: Very high resolution regional climate model simulations over
452 Greenland: Identifying added value, *J. Geophys. Res.,* 117, D02108.
453 Miller, N. B., D. D. Turner, R. Bennartz, M. D. Shupe, M. S. Kulie, M. P. Cadeddu, and V. P.
454 Walden, 2013: Surface-based inversions above central Greenland, *J. Geophys. Res.*
455 *Atmos.*, 118, 495–506, doi:10.1029/2012JD018867.
456 Miller, D.H. 1956. The influence of snow cover on local climate in Greenland. *J.*
457 *Meteorol.*, 13(1), 112–120.

458 Nghiem, S.V., D.K. Hall, T.L. Mote, M. Tedesco, M.R. Albert, K. Keegan, C.A. Shuman, N.E.
459 DiGirolamo, and G. Neumann, 2012: The extreme melt across the Greenland ice sheet
460 in 2012, *Geophys. Res. Lett.,* **39**, L20502.
461 Østby, T. I., Schuler, T. V., and Westermann, S. (2014). Severe cloud contamination of
462 MODIS Land Surface Temperatures over an Arctic ice cap, Svalbard. *Rem. Sens. of Env.*
463 **142**, 95–102. http://dx.doi.org/10.1016/j.rse.2013.11.005
464 Rennermalm, Å., S. Moustafa, J. Mioduszewski, V. Chu, R. Forster, B. Hagedorn, J. Harper,
465 T. Mote, D. Robinson, C.A. Shuman, L. Smith, and M. Tedesco, 2013: Understanding
466 Greenland ice sheet hydrology using an integrated multi−scale approach. *Environ.*
467 *Res. Lett.,* **8**, 1, 015017.
468 Riggs, G.A., D.K. Hall, and V.V. Salomonson, 2006: MODIS snow products user guide.
469 NASA Goddard Space Flight Center, Greenbelt, Maryland, USA. [Online: http://modis-
470 snow-ice.gsfc.nasa.gov/uploads/sug_c5.pdf]
471 Shuman, C.A., K. Steffen, J.E. Box, and C.R. Stearns, 2001: A dozen years of temperature
472 observations at the Summit: Central Greenland automatic weather stations 1987–99.
473 *J. App. Meteor.,* **40**, 741–752.
474 Stearns, C.R., 1996: Automated weather station data for Greenland ice core locations.
475 National Snow and Ice Data Center, Boulder, Colorado, USA. [Online:
476 http://nsidc.org/data/arcss005.html]
477 Steffen, K. and J. Box, 2001: Surface climatology of the Greenland ice sheet: Greenland
478 Climate Network 1995–1999. *J. Geophys. Res.,* **106**, D24, 33,951−33,964.
479 Stroeve, J. and K. Steffen, 1998: Variability of AVHRR−derived clear−sky surface
480 temperature over the Greenland Ice Sheet. *J. App. Meteor.,* **37**, 23–31.

van den Broeke, M.R., P. Smeets, J. Ettema, C. van der Veen, R. van de Wal, and J. Oerlemans, 2008: Partitioning of melt energy and meltwater fluxes in the ablation zone of the west Greenland Ice Sheet. *The Cryosphere,* **2**, 179–189.

van den Broeke, M.R., C.J.P.P. Smeets, and R.S.W. van de Wal, 2011: The seasonal cycle and interannual variability of surface energy balance and melt in the ablation zone of the west Greenland Ice Sheet. *The Cryosphere,* **5**, 377–390.

Wang, X. and J. Key, 2003: Recent trends in Arctic surface, cloud, and radiation properties from space. *Science,* **299**, 1725–1728.

Warren, S. G., and R. E. Brandt, 2008: Optical constants of ice from the ultraviolet to the microwave: A revised compilation*, J. Geophys. Res.,* **113**, *D14220*.

Westermann, S., Langer, M., & Boike, J. (2012). Systematic bias of average winter-time land surface temperatures inferred from MODIS at a site on Svalbard, Norway. *Remote Sensing of Environment,* **118**, 162–167.

Table 1 – Summary statistics for the IST − T_A differences for each year

Year	Points	Min °C	Max °C	Mean °C	Std. Dev. °C	RMS °C
2008* all	222	−27.42	3.08	−3.81	4.01	5.52
2008 filt.*	*200*	*−8.49*	*1.84*	*−3.01*	*2.06*	*3.65*
2009 all	535	−29.72	3.50	−3.44	3.77	5.10
2009 filt.	*490*	*−9.44*	*1.87*	*−2.70*	*2.15*	*3.45*
2010 all	474	−26.46	5.43	−3.75	3.98	5.47
2010 filt.	*418*	*−9.21*	*1.72*	*−2.85*	*2.13*	*3.56*
2011 all	510	−34.78	4.04	−3.89	4.60	6.02
2011 filt.	*448*	*−9.74*	*1.04*	*−2.82*	*2.29*	*3.63*
2012 all	488	−20.57	4.10	−3.48	3.62	5.02
2012 filt.	*442*	*−9.99*	*2.11*	*−2.82*	*2.19*	*3.57*
2013* all	307	−24.73	5.90	−1.96	3.48	3.99
2013 filt.*	*272*	*−9.13*	*2.39*	*−1.88*	*2.42*	*3.06*

*Indicates that the NOAA Logan sensor observations began on 6 July 2008 and data has been compared through 31 August 2013. Each year of data in the comparison were examined before and after applying a ±5 degree regression filter to the data ('all' and 'filt.', respectively). See text for the rationale for applying the filter.

513 **List of Figures**

514 Figure 1 – Scatter plots of the temporally–coincident 2008–2013 IST and T_A data (±3-
515 minute averages). Linear regression lines are shown for all data (red symbols) and a
516 subset of the data (blue symbols) after a ±5°C regression filter was applied. The dashed
517 black line indicates where the two data sets would be equivalent. The rationale for the
518 filter is discussed in the text and the red–only points show the data that were excluded
519 from further study. The blue regression line suggests that the IST–T_A difference is close
520 to −0.5°C at freezing and about −5°C at −60°C. Statistics for overall differences for the
521 plotted data are shown. Generally similar results were obtained for the each year of the
522 study (see Table 1).
523
524 Figure 2 – Scatter plot showing the 2008–2013 T_A variability (the standard deviation of
525 all the values in the ±3-minute average) as a function of the mean temperature. In a few
526 cases, temperature changes exceeding 5°C were documented within these short
527 periods leading to the larger standard deviation values. The 'step' observed in the
528 scatter plot is due to the 0.1°C reported resolution of the NOAA data.
529
530 Figure 3 – Scatter plot of the 2008–2013 IST–T_A differences as a function of the net
531 distance between the MODIS pixel and the NOAA sensor location. A linear regression
532 line shows little variation for data within 3 km. These data had the ±5–degree
533 regression filter applied. The closest IST value was selected if more than one was
534 available from the MODIS swath.
535

Figure 4 – Scatter plot of the 2008–2013 IST–T_A differences as a function of angle between the MODIS sensor and the in situ data. The regression line suggests there is a small decrease in IST as the angle increases. These data had the ±5–degree regression filter applied.

Figure 5 – Scatter plot of the 2008–2013 IST–T_A differences as a function of the solar illumination angle relative to the IST location. The regression line is not an ideal model for these data but suggests there is a distinct decrease in IST relative to T_A as the angle increases. These data had the ±5–degree regression filter applied. Additional structure in the plotted data is discussed in the text.

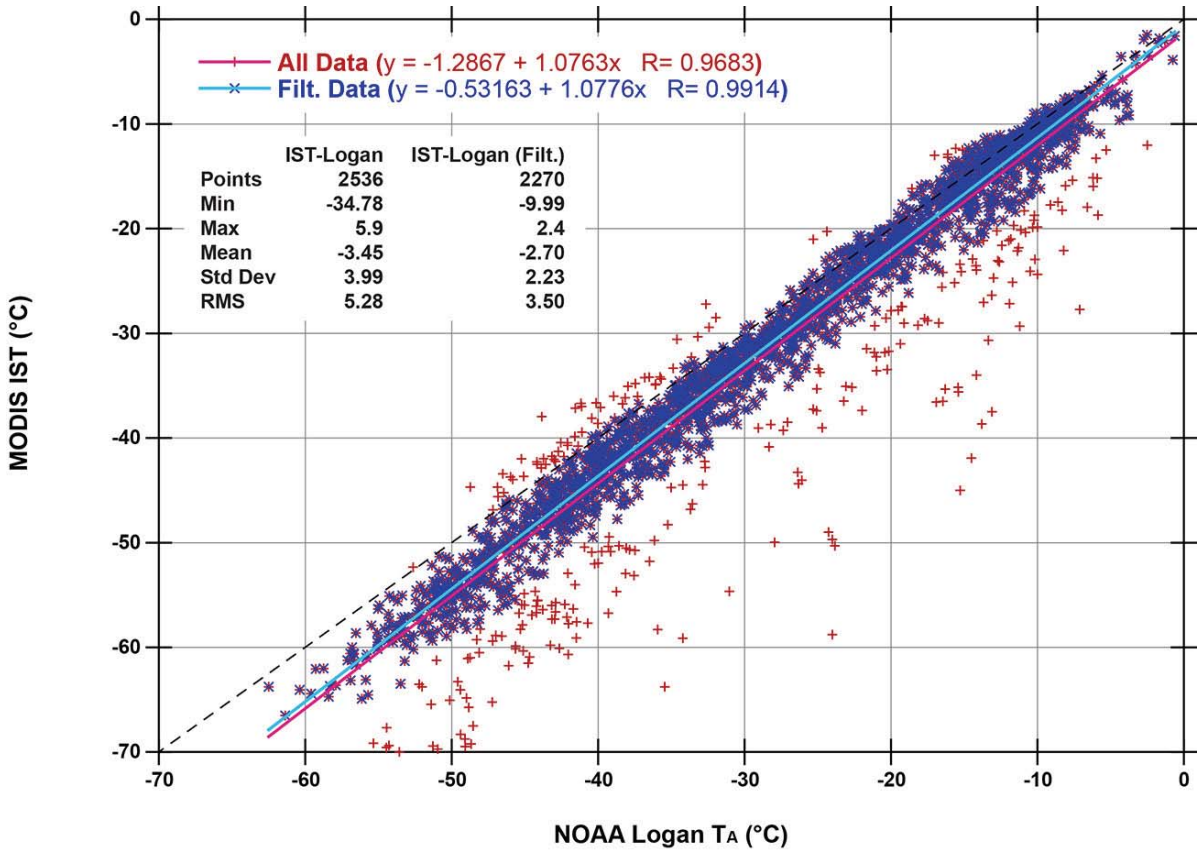

Figure 1 – Scatter plots of the temporally–coincident 2008–2013 IST and T_A data (±3-minute averages). Linear regression lines are shown for all data (red symbols) and a subset of the data (blue symbols) after a ±5°C regression filter was applied. The dashed black line indicates where the two data sets would be equivalent. The rationale for the filter is discussed in the text and the red–only points show the data that were excluded from further study. The blue regression line suggests that the IST–T_A difference is close to –0.5°C at freezing and about –5°C at –60°C. Statistics for overall differences for the plotted data are shown. Generally similar results were obtained for the each year of the study (see Table 1).

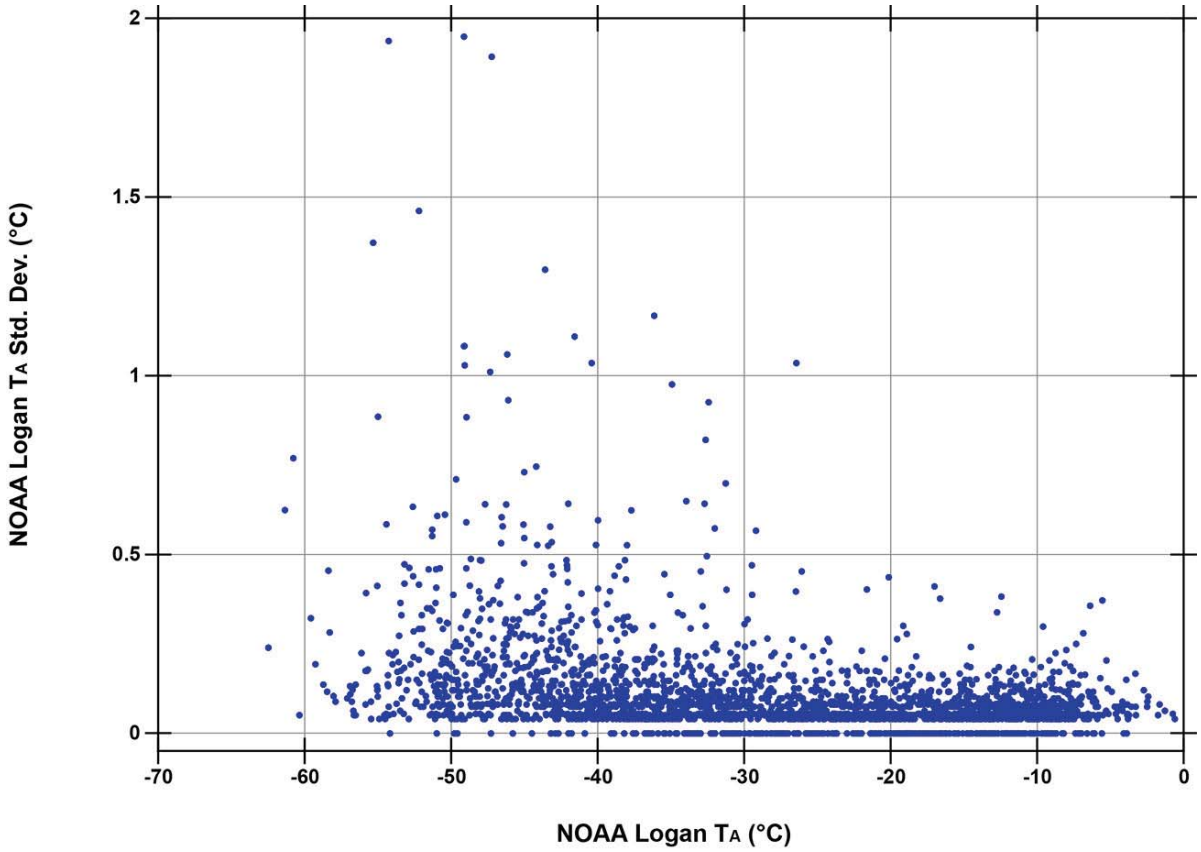

557

558 Figure 2 – Scatter plot showing the 2008–2013 T_A variability (the standard deviation of
559 all the values in the ±3-minute average) as a function of the mean temperature. In a few
560 cases, temperature changes exceeding 5°C were documented within these short
561 periods leading to the larger standard deviation values. The 'step' observed in the
562 scatter plot is due to the 0.1°C reported resolution of the NOAA data.

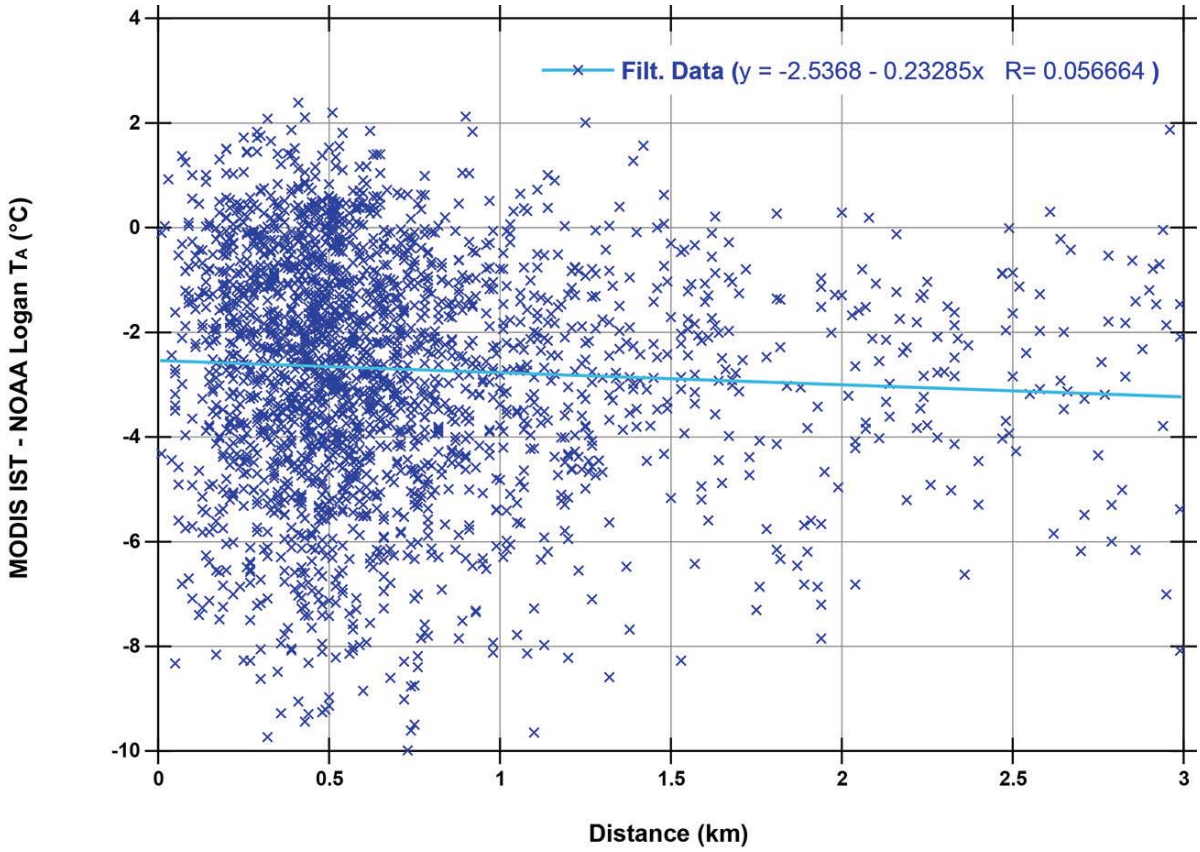

563

564 Figure 3 – Scatter plot of the 2008–2013 IST–T_A differences as a function of the net
565 distance between the MODIS pixel and the NOAA sensor location. A linear regression
566 line shows little variation for data within 3 km. These data had the ±5–degree
567 regression filter applied. The closest IST value was selected if more than one was
568 available from the MODIS swath.

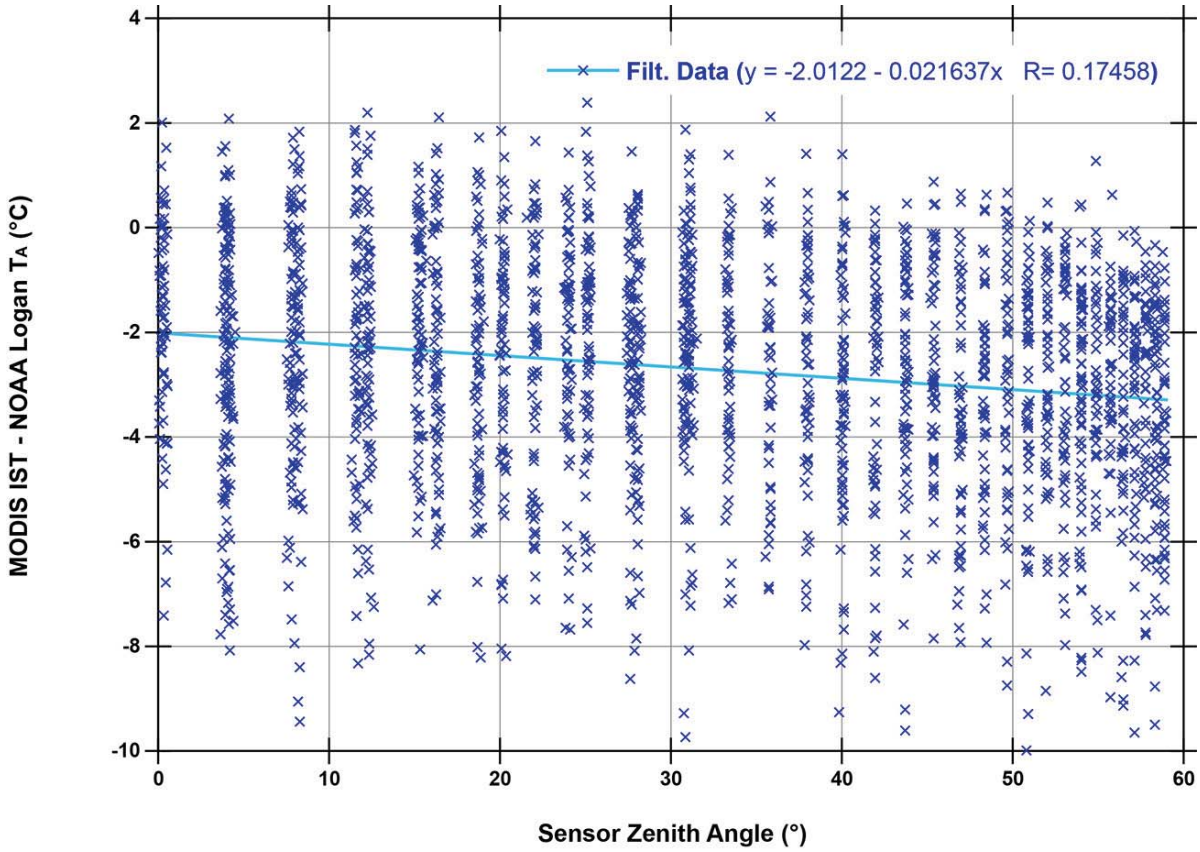

569

570 Figure 4 – Scatter plot of the 2008–2013 IST–T_A differences as a function of angle
571 between the MODIS sensor and the in situ data. The regression line suggests there is a
572 small decrease in IST as the angle increases. These data had the ±5–degree regression
573 filter applied.

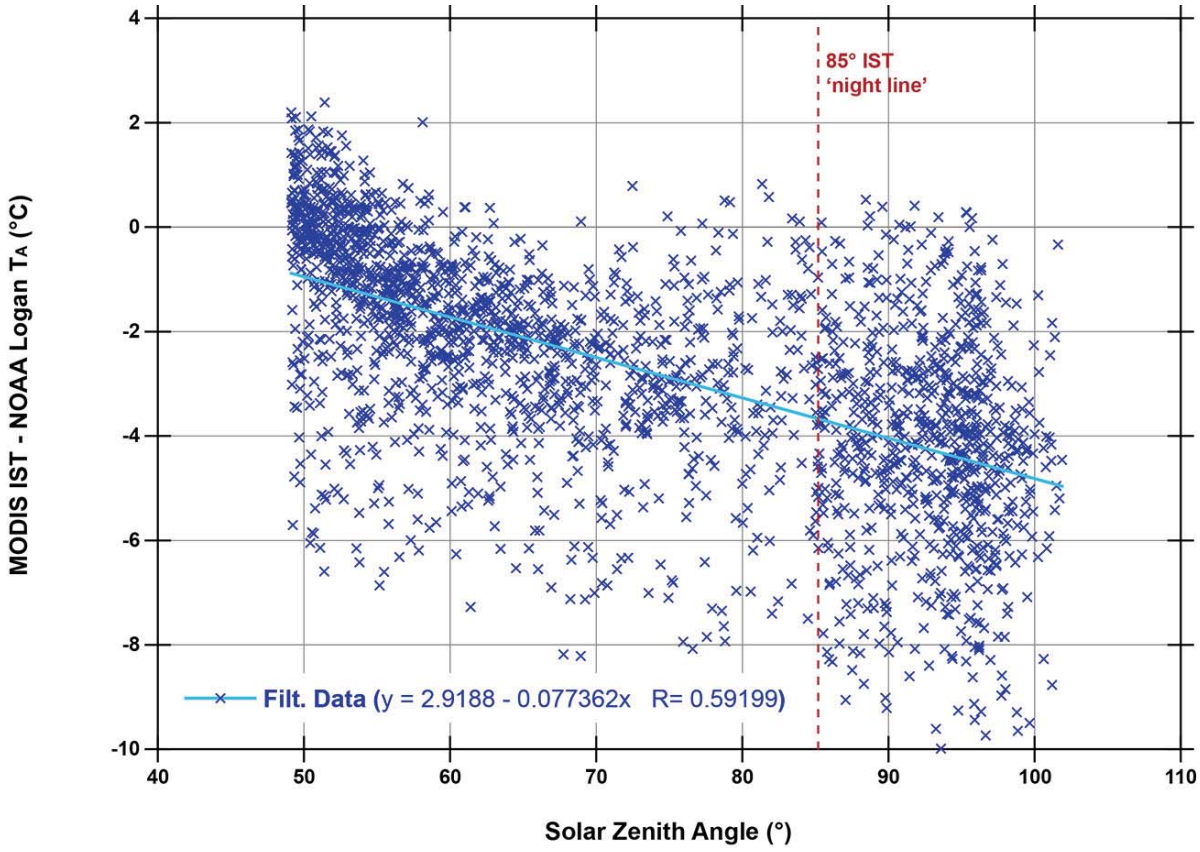

574

575 Figure 5 – Scatter plot of the 2008–2013 IST–T_A differences as a function of the solar
576 illumination angle relative to the IST location. The regression line is not an ideal model
577 for these data but suggests there is a distinct decrease in IST relative to T_A as the angle
578 increases. These data had the ±5–degree regression filter applied. Additional structure
579 in the plotted data is discussed in the text.